ChemComm

Accepted Manuscript

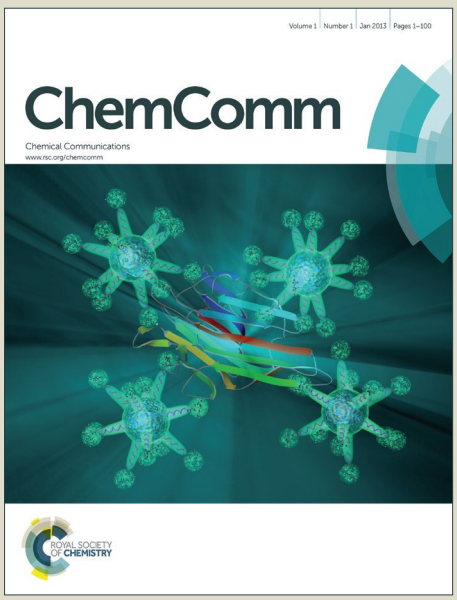

ROYAL SOCIETY OF CHEMISTRY

www.rsc.org/chemcomm

Journal Name

COMMUNICATION

Improved mechanical stability of HKUST-1 in confined nanospace

M.E. Casco,[a] J. Fernández-Catalá,[a] M. Martínez-Escandell,[a] F. Rodríguez-Reinoso,[a] E.V. Ramos-Fernandez,[a] and J. Silvestre-Albero[a,*]

Received 00th January 20xx,
Accepted 00th January 20xx

DOI: 10.1039/x0xx00000x

www.rsc.org/

One of the main concerns in the technological appplication of several metal-organic frameworks (MOFs) relates to their structural instability under pressure (after a conforming step). Here we report *for the first time* that mechanical instability can be highly improved via nucleation and growth of MOF nanocrystals in the confined nanospace of activated carbons.

Metal-organic frameworks (MOFs) have emerged in the last few years as exciting nanomaterials with a very promising performance in a wide range of applications from gas separation and storage,[1-4] to drug delivery and imaging,[5-6] catalysis,[7-9] among others. Despite the high relevance acquired by MOF materials in the field of nanoporous solids and their applications, these nanoporous materials exhibit several drawbacks that must be addressed before they can be successfully applied in any industrial technology. One of the main disadvantages of several MOFs concerns their limited structural stability under pressure, i.e. the structural damage associated with a mechanical compression required in any conforming step.[10,11] For instance, recent studies described in the literature have shown that the structural instability of HKUST-1 can give rise to a drastic decrease in the exceptional performance of this MOF for methane storage at high-pressures (up to 50% decrease after a conforming step at 1.5 Tons).[3,12] Consequently, new MOF materials efficiently packable and retaining the full sorption capacity are required for gas storage applications. Besides MOFs, recently published results from our research group have anticipated that carefully designed activated carbons can also be considered as promising porous materials to reach the new DOE target (263 V/V) for methane storage at high pressures but preserving the structural integrity and adsorption properties after a compressing step.[12]

With this background, the present paper is aimed to take advantage of the privileged structural properties of carbon materials and the exceptional adsorption performance of MOFs via nucleation and growth of MOFs nanocrystals in the inner cavities of carbon materials (Scheme 1). HKUST-1 was selected as a guest structure for the confinement experiments due to its excellent performance for methane adsorption at high pressures. As a host structure, activated carbon (petroleum-pitch activated carbon-AC) has been specifically designed with a highly developed porous structure (containing micro-/meso- and macropores) so that nano-confinement effects in the cavities of carbon materials can be used.[13] The main role of the nanocavities, where enhanced adsorption potential takes place, is i) to promote the growing of MOF nanocrystals and ii) to protect the guest nanostructures from an external stimuli (e.g., mechanical compression). To this end, three hybrid MOF@AC have been prepared containing 10 wt.% (MOF@AC10), 25 wt.% (MOF@AC25) and 50 wt.% (MOF@AC50) of activated carbon. The synthesis was performed according to the recipe described by Hupp et al. for HKUST-1, but modified by the incorporation of a ranging amount of activated carbon in the reaction media (see supporting information for further details).[3] It is important to highlight that the hydrothermal synthesis was performed under continuous stirring to minimize reactant diffusional limitations, thus avoiding preferential growing of the MOF in the external surface of the carbon grains.

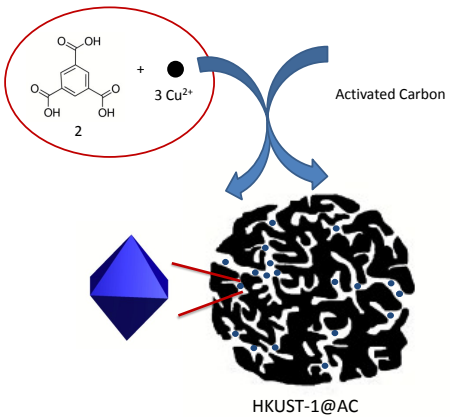

Scheme 1. Schematic representation of the HKUST-1 nanocrystals grown in the inner cavities of activated carbons.

Table 1 reports the textural characteristics of the different hybrid systems in terms of BET surface area, micropore volume (calcula

[a] *Laboratorio de Materiales Avanzados, Departamento de Química Inorgánica-Instituto Universitario de Materiales, Universidad de Alicante, Ctra. San Vicente-Alicante s/n, E-03690 San Vicente del Raspeig, Spain.*
Email: joaquin.silvestre@ua.es; Tel: +34 965909350; Fax: +34 965903454

† Electronic Supplementary Information (ESI) available: [Samples preparation and characterization]. See DOI: 10.1039/x0xx00000x

using the Dubinin-Radushkevich (DR) equation) and total pore volume (at $P/P_0 \sim 0.95$), estimated from the nitrogen adsorption isotherms at -196ºC (nitrogen adsorption isotherms and DR plots are shown in Figure S1a and Figure S1b, respectively). Textural properties of the original HKUST-1 and AC are also included for the sake of comparison. As it can be appreciated in Table 1, textural parameters of the hybrid systems highly resemble the values of the parent MOF in terms of micropore volume and BET surface area, independently of the amount of carbon incorporated. Although these results are quite surprising, they are highly reproducible for other MOFs evaluated by our research group (e.g. ZIF-8@AC).[14] The observed behaviour could be attributed to the larger skeleton density of MOF (helium density 2.80 g/cm^3), as compared to AC (helium density 1.90 g/cm^3), so that the final textural properties per gram of hybrid system are preferentially defined by the MOF matrix.[12] However, further theoretical calculations will be needed to fully understand this behaviour. At this point it is important to highlight the sudden decrease observed in the textural parameters of the parent carbon material (mainly S_{BET}, V_{DR} and V_t) after a 50 wt.% MOF incorporation. This observation clearly suggests that MOF nucleation and growth must take place preferentially in the inner cavities of the activated carbon, although the isolated growing of some MOF crystals in the external surface of the carbon grains cannot be ruled out.

Table 1. Textural properties deduced from the nitrogen adsorption isotherms at -196ºC.

Sample	S_{BET} /m^2·g^{-1}	V_{DR} /cm^3·g^{-1}	V_t /cm^3·g^{-1}
HKUST-1	1590	0.59	0.64
MOF@AC10	1700	0.64	0.88
MOF@AC25	1190	0.44	0.86
MOF@AC50	1600	0.51	1.10
AC	3790	1.19	2.40

V_{DR}, micropore volume deduced from the Dubinin-Radushkevich equation; V_t, total pore volume estimated from the nitrogen adsorption data at $P/P_0 \sim 0.95$.

X-ray powder diffraction measurements of the parent MOF show the characteristic peaks associated to HKUST-1 at 2θ: 9.5, 11.7 and 13.5, corresponding to (220), (222) and (400) diffraction peaks, respectively. Interestingly, encapsulated HKUST-1 exhibits a similar XRD pattern, i.e. there are no shifts in the peaks´ position, although a certain crystallinity loss can be clearly discerned with the amount of carbon incorporated. Despite the similarity in the XRD patterns, it is important to highlight a shift in the relative intensity of the main diffraction peaks of HKUST-1 upon confinement. The (222) diffraction peak experiences a sudden decrease as compared to the (220) and (400) diffraction peaks. This finding may suggest an epitaxial growth of the synthesized nanocrystals in the restricted space of the carbon cavities, this being another sign about HKUST-1 growing in the inner cavities of carbon.

As described above, the main objective of the present paper is the nucleation and growth of HKUST-1 in the cavities of activated carbons to prevent any structural damage or collapse after a mechanical stress. To this end, Figure 2 compares the morphological changes for the original HKUST-1 sample and the hybrid MOF@AC50 system, as synthesized (a,c), and after a conforming step at 1.5 Tons (b,d). The original HKUST-1 presents a heterogeneous particle size distribution with an average crystal size around 360 nm, as deduced from the (222) peak in the XRD measurements using the Scherrer´s equation. It is worth to mention that the particle size obtained under stirring conditions is smaller as compared to the conventional synthesis described in ref. [3].

A conforming step at 1.5 Tons (see Figure 2) gives rise to a compaction of the nanocrystals accompanied by a sudden deterioration of the crystal structure, in close agreement with previous observations.[3,12] The deterioration of the MOF crystal structure after a conforming step is also confirmed by comparing the XRD profiles (see Figure S2).

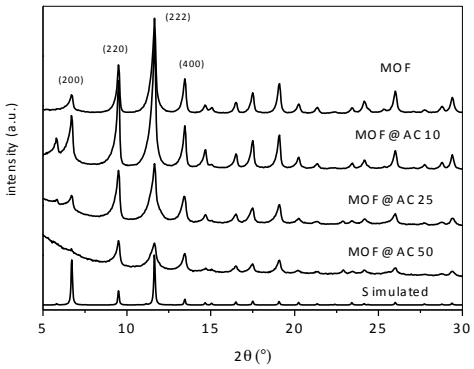

Figure 1. X-ray diffraction pattern of the different hybrid MOF@AC materials. XRD patterns for HKUST-1 synthesized in this work and simulated spectra[15] are included for the sake of comparison.

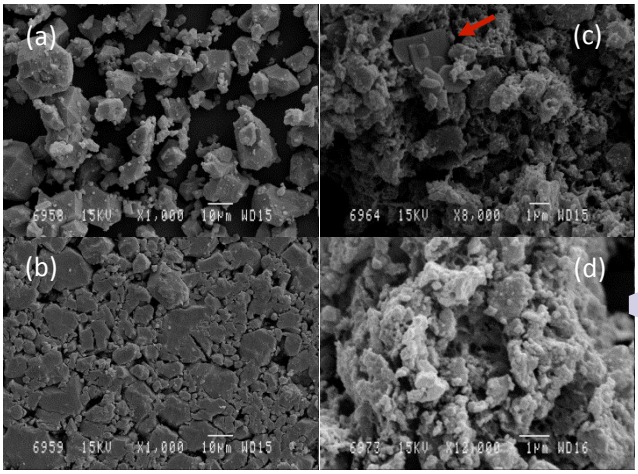

Figure 2. Scanning electron microscopy images of (a,b) MOF (HKUST-1) and (c,d) MOF@AC (50 wt.%) as synthesized (a,c) and after a conforming step at 1.5 Tons (b,d).

Concerning the hybrid system, scanning electron microscopy (SEM) images show the carbon matrix (carbon particle size *ca.* 1-10 μm) and the MOF nanocrystals (red arrow) growing preferentially in the larger cavities (large macropores). Unfortunately, SEM does not provide information about the scenario taken place in narrow pores (mesopores and micropores), where MOF growing is expected (as deduced from N_2 adsorption measurements). The hybrid sample submitted to a mechanical stress at 1.5 Tons (Figure 2d) does not reflect any morphological change or damage, in close agreement with the large structural stability and rigidity of activated carbons as compared to MOFs. The larger stability of the hybrid systems can be clearly appreciated in the XRD patterns obtained after the conforming step (Figure S2).

Another important parameter to define the structural stability of nanoporous materials upon a mechanical stress concerns their textural properties. Figure 3 compares the nitrogen adsorption isotherms at -196ºC for the (a) HKUST-1 sample and (b) hybrid MOF@AC50 after a mechanical compression at 0.5, 1 and 1.5 Tons. As described in our previous studies, the original MOF exhibits an important structural instability associated with a progressive damage of the porous structure upon an external mechanical pressure. For instance, the BET surface area of the HKUST-1 sample exhibits a 43 % decrease (900 m^2/g vs 1590 m^2/g) upon a mechanical conforming at 1.5 Ton, thus confirming the partial collapse of the crystal structure, in close agreement with SEM images.

A completely different scenario accounts for the hybrid samples (e.g., MOF@AC50). The nitrogen adsorption isotherm of the parent hybrid MOF@AC50 system exhibits a type IV, according to the IUPAC classification, clearly resembling that of the host activated carbon (see Figure S1), although with a smaller total adsorption capacity (55% reduction in the total pore volume of the host AC after MOF incorporation). Interestingly, a subsequent conforming step up to 0.5, 1.0 and 1.5 Tons has no effect in the textural properties of the sample. BET surface area, micro- and total pore volume remain mainly unchanged within the experimental error. This observation clearly anticipates *for the first time* the synergetic effect between activated carbons and MOFs, i.e. the protective role of the carbon nanocavities for MOF nanocrystals grown in their bed while preserving the textural properties and adsorption performance of the original MOF (see Figure S3).

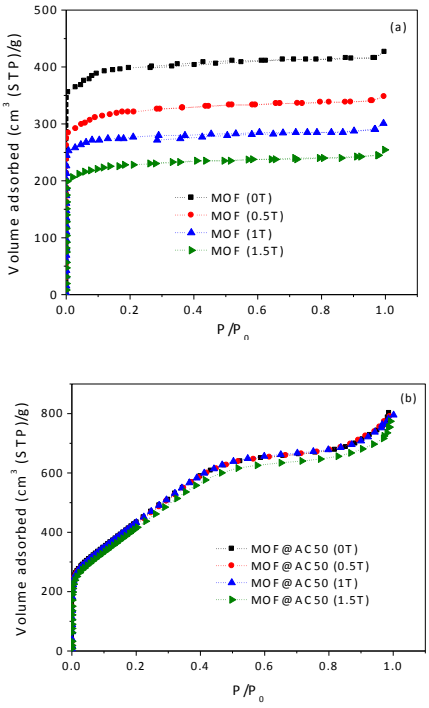

Figure 3. Nitrogen adsorption/desorption isotherms of (a) MOF and (b) MOF@AC (50 wt.%), after a conforming step at 0, 0.5, 1 and 1.5 Tons.

Another proof about the presence of HKUST-1 encapsulated in the porosity of the host carbon material can be obtained from the textural parameters obtained from the nitrogen adsorption measurements. If all the HKUST-1 is outside the carbon material, the total pore volume for the MOF@AC50 detected by nitrogen would be $V_1 = 0.5 \times V_{AC} + 0.5 \times V_{MOF} = 0.5 \times 2.40 + 0.5 \times 0.64 = 1.5$ cm^3/g, which is far from the obtained value ($V_t = 1.10$ cm^3/g). On the contrary, if all HKUST-1 is inside the cavities of the host carbon material, the total adsorption capacity of the carbon must decrease according to the MOF density ($\rho = 0.88$ g/cm^3) but considering the additional contribution from the MOF to the total adsorption capacity, i.e. $V_2 = (0.5 \times V_{AC} - 0.5/\rho) + 0.5 \times V_{MOF} = (0.5 \times 2.40 - 0.5/0.88) + 0.5 \times 0.64 = 0.95$ cm^3/g, in close agreement with the experimental value. This statement confirms that the majority of the HKUST-1 crystals must be located inside the cavities of the carbon material.

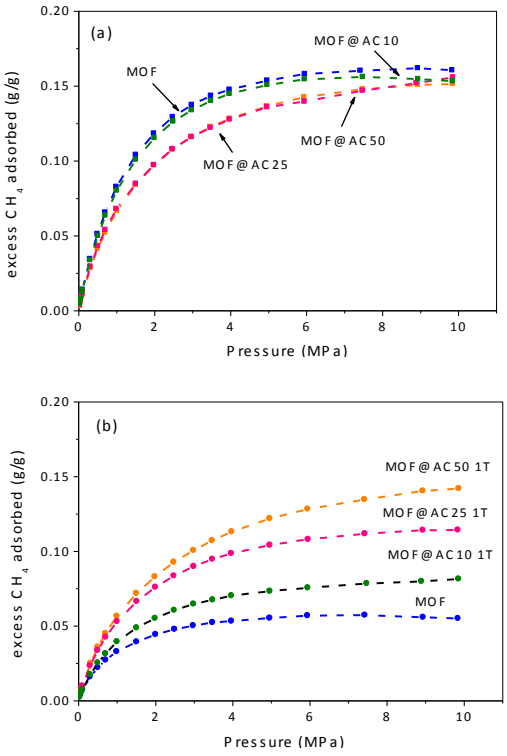

Figure 4. Excess methane adsorption isotherms at 25ºC in the hybrid MOF@AC samples (a) as synthesized and (b) after a conforming step at 1 Ton.

Last but not least, these hybrid materials were evaluated in the adsorption of methane at 25ºC and high-pressure (up to 10 MPa), before and after a conforming step. As described in Figure 4, HKUST-1 (MOF) exhibits a considerable adsorption capacity for methane reaching saturation at around 8 MPa with a final value of 0.16 g/g. It is worth to mention that the amount adsorbed on the HKUST-1 material used in this manuscript is smaller than previous values described in the literature.[3,12] The lower adsorption capacity for methane on the present sample must be attributed to the smaller crystal size (due to the stirring used during the synthesis), thus anticipating the critical role of the crystal size in HKUST-1 for methane storage at high pressures. Confinement of HKUST-1 in the cavities of the activated carbons gives rise to a minor decrease of the methane excess adsorption capacity, mainly at moderate pressures, while the final value at 10 MPa in the amount adsorbed resembles that of the parent MOF (see Table S1 for a compilation of the adsorption data).

A completely different situation takes place after a conforming step at 1 Ton. As observed in Figure 4b, the excess methane adsorbed

drastically drops in the non-confined MOF down to 0.05 g/g, in close agreement with previous observations.[3,12] However, the detrimental effect of a mechanical stress decreases with the amount of carbon in the hybrid system up to sample MOF@AC50, with mainly no effect in the amount of methane adsorbed at 10 MPa (0.14 g/g vs 0.15 g/g). These results constitute the *first proof-of-concept* for MOF protection against an external stimuli (e.g., pressure required for a conforming step), via confinement of the MOF in the nanocavities of activated carbons while preserving the adsorption properties of the non-confined nanocrystals.

To end up, Table 2 compares the methane excess adsorption capacity in volumetric basis (V/V) for the different samples before and after the compressing step. As expected, differences in the methane adsorption capacity become larger among samples in volumetric basis as compared to gravimetric, due to the higher density of HKUST-1 vs the hybrid systems.

Table 2. Excess methane uptake at 10 MPa and 25ºC for the different samples before and after the conforming step. Volumetric capacity (V/V) has been calculated using the bulk density measured at 1.0 Ton (also included in the Table).

Sample	ρ ($g \cdot cm^{-3}$)¥	Excess Methane (10 MPa, 25ºC)	Excess Methane (10 MPa, 25ºC)*
MOF	0.88	198 V/V	68 V/V
MOF@AC10	0.83	179 V/V	95 V/V
MOF@AC25	0.75	163 V/V	119 V/V
MOF@AC50	0.63	134 V/V	126 V/V

¥ Bulk density measured at 1.0 Ton; * Excess Methane after a conforming step at 1.0 Ton.

The excess methane adsorbed in the as-synthesized samples decreases with the amount of carbon incorporated from 198 V/V down to 134 V/V (using erroneously the bulk density measured at 1.0 Ton when the sample is already damaged). As described before, the volumetric adsorption capacity is larger for the large crystals of HKUST-1 (257 V/V according to our previous measurements in ref. 10), as compared to the new sample prepared under stirring conditions. In the same way as before, the scenario changes drastically after the conforming of the different samples. Non-confined MOF suffers a dramatic reduction in the methane excess adsorption capacity down to 68 V/V, whereas the confined samples (preferentially MOF@AC50 sample) do not. At this point it is important to emphasize that despite these advantages, hybrid MOF@AC systems will never outperform the adsorption performance of the parent MOF, at least in crystal size dependent applications such as methane adsorption, due to the hindered growing of the MOF in the restricted nanospace of carbon cavities.

In summary, this manuscript describes the nucleation and growth of HKUST-1 nanocrystals in the cavities of carefully designed activated carbon materials. Gas adsorption measurements suggest that nucleation and growth of MOF nanocrystals must take place preferentially in the confined nanocavities of the carbon material, as confirmed by microscopy. Confinement of MOF nanocrystals provides a considerable improvement in the mechanical properties of the MOF due to the protective barrier of the host carbon against a mechanical stress, while preserving the excellent adsorption properties of the guest MOF. Whereas the porous structure of isolated HKUST-1 sample exhibits a drastic structural collapse after a mechanical stress at 1 Ton, hybrid systems are able to withstand higher pressures without any significant modification in the adsorption properties of the confined MOF.

Financial support from MINECO projects: MAT2013-45008-p and CONCERT Project-NASEMS (PCIN-2013-057) is gratefully acknowledged.

Notes and references

1 K. Sumida, D.L. Rogow, J.A. Mason, T.M. McDonalds, E.D. Bloch, Z.R. Herm, T.-H. Bae, J.R. Long, *Chem. Rev.*, 2012, **112**, 724.
2 A.R. Millward, O.M. Yaghi, *J. Am. Chem. Soc.*, 2005, **127**, 17998.
3 Y. Peng, V. Krungleviciute, I. Eryazici, J.T. Hupp, O.K. Farha, T. Yildirim, *J. Am. Chem. Soc.*, 2013, **135**, 11887.
4 I. Senkovska, S. Kaskel, *Microp. Mesop. Mater.*, 2008, **112**, 108.
5 P. Horcajada, C. Serre, G. Maurin, N.A. Ramsahye, F. Balas, M. Vallet-Regí, M. Sebban, F. Taulelle, G. Ferey, *J. Am. Chem. Soc.*, 2008, **130**, 6774.
6 P. Horcajada, T. Chalati, C. Serre, B. Gillet, C. Sebrie, T. Baati, J.F. Eubank, D. Heurtaux, P. Clayette, C. Kreuz, J.-S. Chang, Y.K. Hwang, V. Marsaud, P.-N. Bories, L. Cynober, S. Gil, G. Ferey, P. Couvreur, R. Gref, *Nature Mater.*, 2010, **9**, 172.
7 J.Y. Lee, O.K. Farha, J. Roberts, K.A. Scheidt, S.T. Nguyen, J.T. Hupp, *Chem. Soc. Rev.*, 2009, **38**, 1450.
8 J. Gascon, A. Corma, F. Kapteijn, F.X. Llabrés i Xamena, *ACS Catal.*, 2014, **4**, 361.
9 B. Gole, U. Sanyal, P.S. Mukherjee, *Chem. Commun.*, 2015, DOI: 10.1039/c4cc09228g.
10 J. Chong Tan, A.K. Cheetham, *Chem. Soc. Rev.*, 2011, **40**, 1059.
11 T. Tian, J. Velazquez-Garcia, T.D. Bennett, D. Fairen-Jimenez, *J. Mater. Chem. A*, 2015, **3**, 2999.
12 M.E. Casco, M. Martinez-Escandell, E. Gadea-Ramos, K. Kaneko, J. Silvestre-Albero, F. Rodriguez-Reinoso, *Chem. Mater.* 2015, **27**, 959.
13 M.E. Casco, J. Silvestre-Albero, A.J. Ramirez-Cuesta, F. Rey, J.L. Jorda, A. Bansode, A. Urakawa, I. Peral, M. Martinez-Escandell, K. Kaneko, F. Rodriguez-Reinoso, *Nature Commun.*, 2015, **6**, 6432.
14 M.E. Casco, D. Fairen-Jimenez, A.J. Ramirez-Cuesta, L. Daeman, E.V. Ramos-Fernandez, J. Silvestre-Albero, *unpublished results*
15 Simulated XRD pattern obtained from http://www.crystallography.net/cod/2300380.html, accessed on July 14th 2015.